Convertible modes of inactivation of potassium channels in *Xenopus* myocytes differentiating *in vitro*

Uwe Ernsberger and Nicholas C. Spitzer*

Department of Biology and Center for Molecular Genetics, University of California, San Diego, La Jolla, CA 92093-0357, USA

1. Voltage-dependent inactivating single-channel potassium currents were recorded in cell-attached and inside-out patches from embryonic *Xenopus* myocytes differentiating in culture.

2. Channels with rapid inactivation (time constants < 25 ms) and with slow inactivation (time constants > 80 ms) recorded after one day *in vitro* appear to belong to two functionally different classes. Rapidly and slowly inactivating channels show steady-state inactivation with potentials of half-inactivation of -74 ± 7 and -44 ± 9 mV. They exhibit voltage-dependent activation, with times to half-maximal activation of $0{\cdot}79 \pm 0{\cdot}09$ and $1{\cdot}17 \pm 0{\cdot}22$ ms when stepped from −120 to +40 mV. Rapidly inactivating channels also have a lower open probability than slowly inactivating ones. The channels have similar conductances of 23 ± 6 and 17 ± 4 pS and extrapolated reversal potentials close to the potassium equilibrium potential.

3. In cell-attached patches, inactivation behaviours of channels with rapid or slow inactivation do not change during recording. After patch excision, rapidly inactivating channels usually switch to a slow inactivation mode. Slowly inactivating channels derived from rapidly inactivating channels after patch excision retain their conductance and extrapolated reversal potential, but are not distinguishable from native slowly inactivating channels with respect to steady-state inactivation, activation and inactivation times, as well as open probabilities.

4. The change in inactivation behaviour of rapidly inactivating channels after patch excision is reversed by application of reduced dithiothreitol (DTT). In contrast, channels with slow inactivation in the cell-attached mode do not change into rapidly inactivating channels after application of DTT in the excised configuration, suggesting that these channels belong to a structurally different class.

5. Frequent observation of superposing channel openings indicates clustering of inactivating potassium channels in the myocyte membrane, since many patches lack channel activity. Clustering does not depend on the presence of differentiating neurones.

6. Channels with rapid inactivation increase 6-fold in density during the first day in culture in the presence of neurones; channel density decreases in their absence. Channels with slow inactivation increase 2-fold in density in the presence or absence of differentiating neurones during this period.

7. Channels with rapid or slow inactivation in cell-attached membrane belong to functionally distinct classes that are developmentally regulated differently. Reversible changes from rapid to slow inactivation mode after patch excision suggest that the channels may be structurally related.

In recent years an increasing number of functionally distinct potassium channels have been described (Rudy, 1988). With molecular characterization of the *Shaker* locus in *Drosophila*, encoding voltage-dependent potassium channels (Jan & Jan, 1992), the functional diversity of potassium channels began to be understood in terms of differences in amino acid sequence of the channel proteins.

* To whom correspondence should be addressed.

In addition to the potassium channel gene at the *Shaker* locus, other genes have been described in *Drosophila* that encode voltage-dependent potassium channels giving rise to currents of the rapidly inactivating A type or the delayed rectifier type (Wei, Covarrubias, Butler, Baker, Pak & Salkoff, 1990). Differences in kinetic properties indicate that they constitute functionally as well as structurally distinct classes of voltage-dependent potassium channels. Homologues of these channels have been found in vertebrates and assigned to channel classes established for *Drosophila* potassium channel genes according to sequence homology (Wei *et al.* 1990). However, channels assigned to one class may have different kinetic properties. *Drosophila Shaker* channels exhibit inactivating A-like currents (Timpe, Jan & Jan, 1988), whereas at least some rat cortex potassium (RCK) channels, which are grouped in the *Shaker* class by sequence homology, produce delayed rectifier-like currents when expressed in *Xenopus* oocytes (Stühmer *et al.* 1989).

In striated muscle of *Rana*, a voltage-dependent potassium current with similarities to the delayed rectifier current of squid axon has been recorded that inactivates during extended voltage steps (Adrian, Chandler & Hodgkin, 1970*a*; Stanfield, 1970). A corresponding delayed rectifier-like current has been observed during the initial stages of muscle development in *Xenopus* myocytes differentiating *in vitro* (Ribera & Spitzer, 1991) in addition to rapidly inactivating potassium A-like currents (Ribera & Spitzer, 1991; Moody-Corbett & Gilbert, 1992; Spruce & Moody, 1992).

Here we describe single voltage-dependent potassium channels expressed in myocytes differentiating from cultured *Xenopus* mesodermal cells. A population of slowly inactivating channels had properties expected for a delayed rectifier. In addition, rapidly inactivating channels with properties of potassium A channels are present early during development. The kinetic properties of the latter channels change after patch excision such that they cannot be distinguished from the former delayed rectifier-like channels. The observations suggest that the difference between these A- and delayed rectifier-like channels does not necessarily reside in the primary structure of the channel protein but may be mediated by post-translational modification. Preliminary accounts of some of these findings have been published (Ernsberger & Spitzer, 1990, 1991).

METHODS

Cell cultures

Cultures were prepared from stage 15 *Xenopus* embryos (Nieuwkoop & Faber, 1956) as described previously (Ribera & Spitzer, 1991), conforming to National Institutes of Health guidelines for anaesthesia. In brief, the posterior half of the neural plate region was excised, including underlying meso- and endoderm. Tissue was dissociated into single cells by incubation for 30 min in Ca^{2+}–Mg^{2+}-free Steinberg's solution with the following composition (mM): 116·4 NaCl, 0·7 KCl, 0·4 EDTA, 4·6 Tris, at pH 7·8. Dissociated cells were plated using a glass pipette onto Costar tissue culture plastic in Steinberg's solution, composition (mM): 116·4 NaCl, 0·7 KCl, 1·31 $MgSO_4$, 10 $CaCl_2$, 4·6 Tris, at pH 7·8. Myocytes began to differentiate morphologically after only a few hours; neurones differentiated after ~6 h in culture. These cultures are referred to as 'mixed'. Alternatively, neurone-free cultures were obtained by incubating the tissue in Collagenase A (1 mg ml^{-1}; Boehringer-Mannheim) for 20 min. This treatment allowed separation of mesoderm from ectoderm and endoderm. The mesoderm was then incubated for 15 min in Ca^{2+}–Mg^{2+}-free Steinberg's solution before plating. In these cultures, which are referred to as 'enriched', myocytes constitute the only morphologically differentiating cell type. Recordings were performed 9–12 and 20–30 h after plating (early and late, respectively). Data presented are from recordings during late stages unless indicated otherwise. Biophysical properties of channels observed in myocytes grown in the presence or absence of neurones were similar and the data were not treated separately.

Electrophysiological experiments

Single-channel patch clamp recordings were obtained from cell-attached and excised, inside-out patches of myocyte membrane using pipettes made from Drummond haematocrit capillary tubes (i.d., 1·1 mm; o.d., 1·5 mm). Fire-polished and Sylgard-coated (Dow Corning) pipettes had resistances of 15–25 MΩ; in preliminary experiments 5–10 MΩ pipettes were used. Pipettes were filled with a nominally Ca^{2+}-free solution of composition (mM): 20 KCl, 60 NaCl, 5 $MgCl_2$, 5 Hepes, at pH 7·4. In some experiments, the potassium concentration was reduced to 10 mM by replacing KCl with an equimolar amount of NaCl. To investigate the biophysical properties of ion channels, culture medium was replaced with a bath solution high in potassium to clamp the membrane potential to a value close to 0 mV in cell-attached recordings, and to achieve an ion composition similar to that of the cytoplasm in inside-out recordings. This solution contained (mM): 100 KCl, 3 NaCl, 10 Hepes, 10 EGTA, adjusted to pH 7·4 with KOH, increasing $[K^+]$ to 127 mM (Harris, Henderson & Spitzer, 1988). Assuming an internal potassium concentration of 99 mM, the resting potential in *Xenopus* muscle cells was calculated to be 6·3 mV in this solution (Spitzer, 1976). In vesicles from skeletal muscle of adult *Rana*, the resting potential in a bath solution containing 120 mM KCl was 2·4 mV (Standen, Stanfield, Ward & Wilson, 1984). Therefore, the resting potential was close to 0 mV and voltages given in the text are the inverse of the applied pipette potential. In experiments to determine channel density, the pipette solution was also used as bath solution, giving a concentration of 20 mM KCl on the outside of the patch and the non-patch membrane. Under these recording conditions, the resting membrane potential can be expected to reside near −40 mV (Spitzer, 1976).

In some experiments, bath solution with 10 mM 4-aminopyridine (pH 7·4) was used. In other experiments excised inside-out patches were perfused with bath solution containing 1–10 mM dithiothreitol (DTT; Calbiochem). DTT was used in its reduced or oxidized form, and solutions were freshly made up at the beginning of each experiment. For experiments involving DTT,

127 mM KCl–4% agar bridges were used since 10 mM DTT otherwise shifted the tip potential by >40 mV.

Voltage clamp, data acquisition and data analysis were performed with a DEC PDP 11/23 computer. Initial experiments were done with a Dagan 8900 amplifier (Dagan) using a 10 GΩ headstage. For the majority of experiments, an EPC-7 amplifier (List Electronic) with a 50 GΩ headstage was used. Recorded current signals were filtered at 2·5 kHz and sampled at intervals of 100 μs to several milliseconds.

Data analysis

Current records were obtained during depolarizing voltage commands lasting 20 ms to several seconds. Single-channel conductances (γ) as well as extrapolated reversal potentials (E_{rev}) were obtained from mean current amplitudes at different step potentials by linear regression fits. At least three different voltages were sampled and thirty or more channel openings, of sufficient duration to exclude truncation due to filtering, were generally used to determine mean current amplitudes for each channel. Ensemble average currents were obtained from currents recorded while repeatedly depolarizing from holding to step potential with different prepulse regimes (see Results). Leak and capacitative currents were obtained from current records without channel openings and were digitally subtracted from current traces before creating ensemble average currents. Steady-state inactivation was evaluated by depolarizing patches from various prepulse potentials; experimental values were fitted to the Boltzmann relation using Sigmaplot software (Jandel). Fits of decay of ensemble average currents by exponentials (τ_D), determination of time to half-maximal activation of ensemble average currents ($t_{½,max}$) and binomial analysis were performed as previously described (Harris *et al.* 1988; Hussy, 1991). Open probability (P_o) was determined from the peak amplitude of ensemble average currents, the number of active channels in the patch and the amplitude of unitary currents of active channels at given step potentials. Statistical significance was evaluated by Student's t test or Snedecor's F test (Byrkin, 1987) and the Kolmogorov–Smirnov test (Daniel, 1978). Values are presented as means ± standard deviation for the number of patches indicated in parentheses.

RESULTS

Biophysical properties of potassium channels

Inactivating ensemble average currents of two classes of outward current channels

Depolarization activates a population of inactivating channels carrying outward current in membrane patches from *Xenopus* myocytes grown *in vitro*. When depolarized from strongly negative holding potentials, the majority of channels in cell-attached patches from late myocytes (recorded 20–30 h after plating) activated and inactivated rapidly (Fig. 1*A*), giving rise to ensemble average currents typical for potassium A currents. After excision of a patch the activity persisted (Fig. 1*B*), showing no immediate change in inactivation behaviour. The decay phase of ensemble average currents was fitted with single exponentials having time constants (τ_D) ranging from 2 to 25 ms. Even though these channels may have shown repeated openings during individual depolarizing pulses, this behaviour was so infrequent that it was not manifested as a slowly inactivating component of ensemble average currents.

In addition, a second class of channels was observed in cell-attached as well as excised mode; these channels reopened frequently during a depolarizing pulse (Fig. 2). After a series of openings composed of bursts separated by longer closures, these channels also closed for the

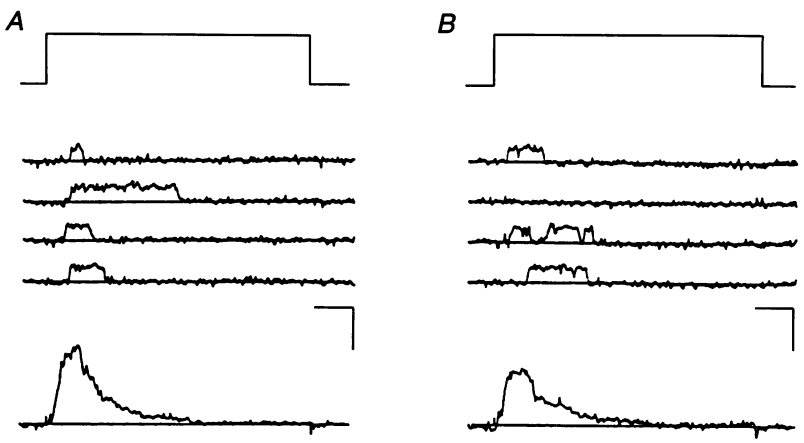

Figure 1. Activity of rapidly inactivating channels observed in a cell-attached and subsequently excised patch containing a single channel

A, cell-attached mode. *B*, the same patch following excision. Here and in subsequent figures the top trace shows the voltage protocol. For *A* and *B*, channel openings during 4 consecutive voltage steps from −100 to +40 mV (0·8 Hz, upper 4 current traces); ensemble average current (60 steps, bottom trace). Horizontal scale: 2·5 ms; vertical scale: 5 (single-channel currents) or 0·5 pA (ensemble average currents). Recordings from a myocyte in a mixed culture at 24 h *in vitro*.

remainder of the voltage step. Long closures at the end of extended voltage steps are likely to represent an inactivated state, as suggested by decay of ensemble average currents and steady-state inactivation (see below). In many cases the decay phase of ensemble average currents was fitted with a single exponential ranging from 80 to 2000 ms. These channels exhibited rapid inactivation only infrequently in cell-attached patches. Two or more exponentials could be required for patches containing several channels, some with a time constant <25 ms and others with a time constant >80 ms.

Single-channel conductance, potassium selectivity and 4-aminopyridine block

Single-channel conductance was determined in cell-attached as well as inside-out patches from late myocytes recorded with $[K^+]_i$ of 127 mM (bath solution) (Fig. 3).

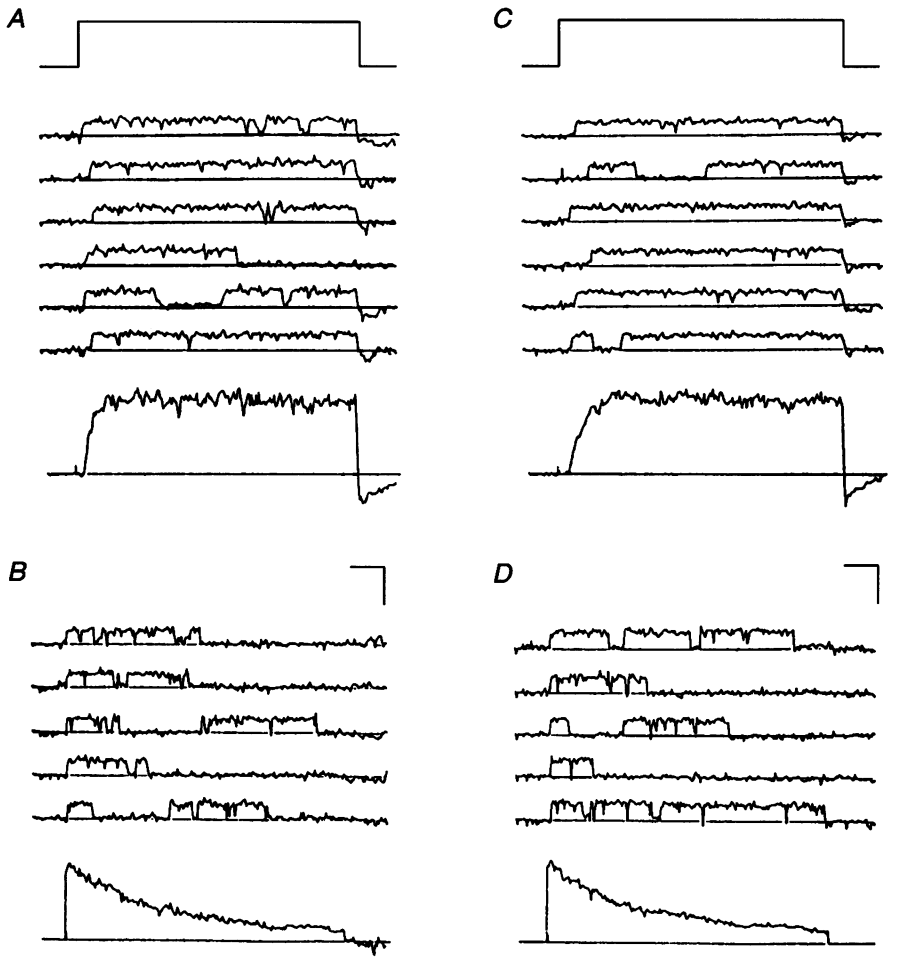

Figure 2. Activity of slowly inactivating channels observed in cell-attached and excised patches containing a single channel

A and *B* show recordings from a slowly inactivating channel in cell-attached mode. *A*, no apparent inactivation during 20 ms depolarizing steps. Channel openings during 6 consecutive voltage steps from −80 to +40 mV (0·8 Hz, upper 6 current traces); ensemble average current (90 steps, bottom trace). *B*, inactivation is apparent during 800 ms depolarizing voltage steps. Voltage protocol as for *A*; channel openings during 5 consecutive voltage steps from −120 to +40 mV (0·8 Hz, upper 5 traces); ensemble average current (124 steps, bottom trace). *C* and *D* show recordings from a slowly inactivating channel in excised mode. *C*, no apparent inactivation during 20 ms depolarizing steps. Channel openings during 6 consecutive voltage steps from −70 to +40 mV (0·8 Hz, upper 6 current traces); ensemble average current (60 steps, bottom trace). *D*, inactivation is apparent during 800 ms depolarizing voltage steps. Voltage protocol as for *C*; channel openings during 5 consecutive voltage steps from −120 to +40 mV (0·8 Hz, upper 5 current traces); ensemble average current (91 steps, bottom trace). Horizontal scale: 2·5 (*A* and *C*) or 100 ms (*B* and *D*); vertical scale: 5 (single-channel currents), 0·5 (ensemble average curents in *A* and *B*) or 1 pA (ensemble average currents in *C* and *D*). Recordings from myocytes in an enriched culture at 25 h (*A* and *B*) and in a mixed culture at 29 h (*C* and *D*) *in vitro*.

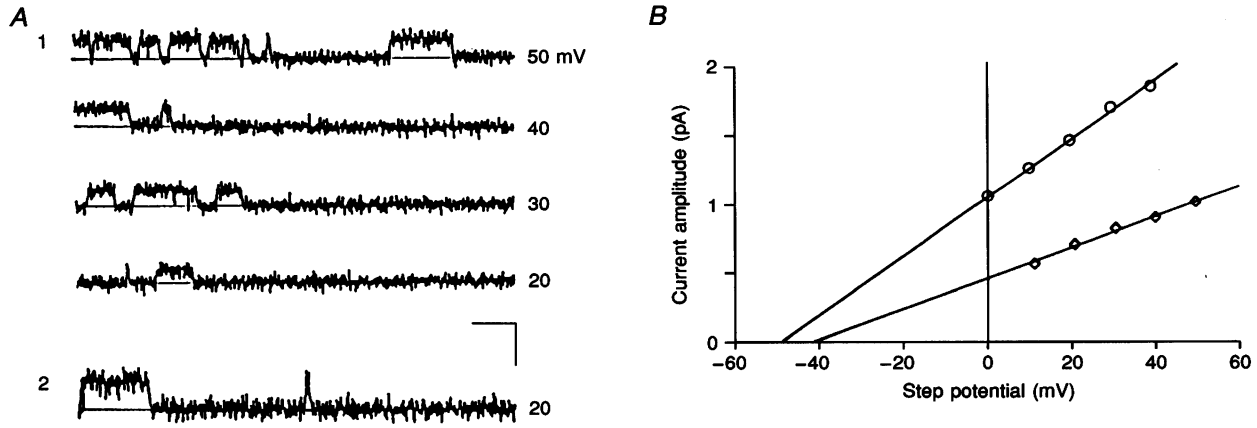

Figure 3. Channels exhibit a range of conductances and are potassium selective

A, activity in 2 excised patches with slowly inactivating channels, assessed as in Fig. 2. First patch, upper 4 traces; second patch, bottom trace. Currents recorded during steps to indicated potentials. The amplitude of unitary currents at +20 mV differs ~3-fold. Horizontal scale: 40 (upper traces) or 20 ms (bottom trace); vertical scale: 2·5 pA. Records from myocytes in enriched cultures at 20 (patch 1) and 28 h (patch 2) *in vitro*. *B*, mean amplitude of unitary currents of slowly inactivating channels recorded in cell-attached mode plotted as a function of voltage. Linear regression yields conductances of 11 and 21 pS and extrapolated reversal potentials of −42 and −48 mV (potassium equilibrium potential, $E_K = -47$ mV). Records from myocytes in enriched cultures at 22 (11 pS channel) and 25 h (21 pS channel) *in vitro*.

Slope conductance was obtained from linear regression of mean current amplitudes at different step potentials for individual channels. In cell-attached patches, conductances were 23 ± 6 pS ($n = 8$) for rapidly inactivating channels and 17 ± 4 pS ($n = 7$) for slowly inactivating channels. Similar values were observed in the excised configuration when recorded with $[K^+]_o$ of 10 or 20 mM. No difference was observed for the conductance of rapidly and slowly inactivating channels under either recording condition (Tables 1 and 2).

The ion selectivity of channels in excised patches was assessed from extrapolated reversal potentials obtained by linear regression fitting of unitary current amplitudes. When $[K^+]_o$ was 20 or 10 mM ($[K^+]_i$, 127 mM), extrapolated reversal potentials for rapidly and slowly inactivating channels were close to the potassium equilibrium potentials (−47 and −65 mV, respectively; Table 1). No difference was observed between the two channel classes. The data indicate that both rapidly and slowly inactivating channels were highly selective for potassium ions.

Blockade of inactivating potassium channels is often achieved with 4-aminopyridine (4-AP), acting from the intracellular side (Howe & Ritchie, 1991). Activity of rapidly and slowly inactivating potassium channels in excised inside-out membrane patches of 1-day-old myocytes was completely blocked in a bath solution containing 10 mM 4-AP. No channel activity was recorded in twenty-eight excised patches. In corresponding experiments without the blocker, 28 and 26% of patches had rapidly and slowly inactivating channels, respectively. The findings are in agreement with recordings in the whole-cell configuration from embryonic *Xenopus* muscle cells, in which 2·5 mM 4-AP reduced the peak and late components of the voltage-dependent outward current partially but not completely (Moody-Corbett & Gilbert, 1992).

Table 1. Conductance (γ) and extrapolated reversal potential (E_{rev}) of potassium channels in excised patches of late myocytes

		Fast ($\tau_D < 25$ ms)		Slow ($\tau_D > 80$ ms)	
$[K^+]_o$ (mM)	E_K (mV)	γ (pS)	E_{rev} (mV)	γ (pS)	E_{rev} (mV)
20	−47	23 ± 4 (5)	−41 ± 6 (5)	18 ± 5 (5)	−50 ± 13 (5)
10	−65	19 ± 4 (3)	−63 ± 6 (3)	16 ± 5 (6)	−68 ± 8 (6)

Fast and Slow refer to the type of inactivation. Data are given as means ± S.D. for the number of patches in parentheses.

Steady-state inactivation of ensemble average currents

The amplitude of ensemble average currents of rapidly inactivating channels decreased with depolarizing holding potentials (Fig. 4*A* and *B*). The rate of recovery from inactivation was determined from ensemble average currents obtained by repeatedly depolarizing patches from −120 or −100 to +40 mV at different pulse frequencies. The increase in peak amplitude of ensemble average currents with increasing interpulse intervals (Fig. 4*C*) could be fitted with a single exponential with a time constant of 0·3 s when the holding potential was −120 (Fig. 4*D*) or −100 mV (data not shown).

Steady-state inactivation of channels in late myocytes was then determined from ensemble average currents obtained by repeatedly depolarizing cell-attached patches containing channels of one inactivation type to +40 mV for 20 ms. Preceding the depolarizing pulse, patches were held for 2·4 s at various prepulse potentials ranging between −120 and −20 mV after holding for 1·2 s at

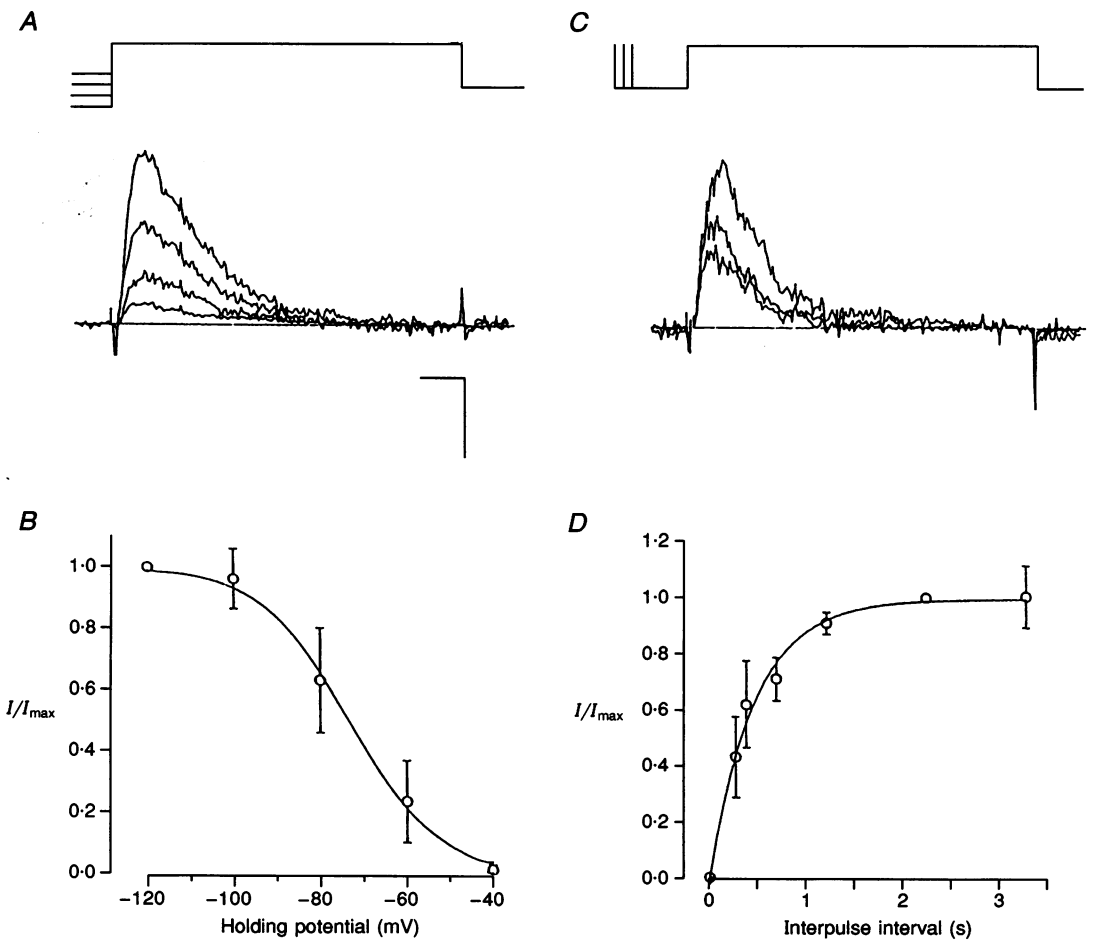

Figure 4. Rapidly inactivating channels inactivate and recover from inactivation

A, ensemble average currents from an excised patch decrease in amplitude with increasingly depolarized holding potentials. The patch was repeatedly stepped to +40 mV at 0·8 Hz with 50 or more steps at each potential. Holding potentials: −120, −110, −100 and −80 mV. Horizontal scale: 2·5 ms; vertical scale: 2·5 pA. *B*, steady-state inactivation of rapidly inactivating channels recorded in cell-attached patches. Peak amplitudes of ensemble average currents are expressed relative to peak amplitude of the current (I/I_{max}) obtained with steps from −120 to +40 mV. Data are fitted with the Boltzmann relation. Patches were held at −100 mV for 1·2 s and stepped to the indicated prepulse potentials for another 2·4 s before the 20 ms test pulse to +40 mV. Records are from myocytes in mixed and enriched cultures at 20–30 h *in vitro*. Data are means ± S.D. ($n = 4$). *C*, ensemble average currents from a cell-attached patch increase in amplitude with decreasing pulse frequency. Patches were repeatedly depolarized from −120 to +40 mV (50 or more pulses at each frequency), at 3·7, 2·6 and 0·8 Hz. Horizontal scale: 2·5 ms; vertical scale: 1 pA. *D*, peak amplitudes of ensemble average currents are expressed relative to the peak amplitude of the current obtained at 0·45 Hz (I/I_{max}) for cell-attached patches. Data are means ± S.D. ($n = 4$). A single exponential fit yields a time constant of 0·3 s. All records from myocytes in mixed cultures at 20–30 h *in vitro*.

−100 mV. Rapidly inactivating channels were fully activated when depolarized from a prepulse potential of −120 mV and completely inactivated at −40 mV (Fig. 4*B*). The potential of half-inactivation was −74 ± 7 mV (the slope factor of the Boltzmann relation, $k = 8{\cdot}9$; Table 2). This value is different from that reported for the peak outward current recorded in whole-cell configuration in embryonic *Xenopus* muscle cells (−40 mV; Moody-Corbett & Gilbert, 1992); the discrepancy may be due to the presence of a slowly inactivating component in whole-cell recordings. In patches containing both rapidly and slowly inactivating channels, the rapidly inactivating component of the ensemble average currents was not well resolved from the slowly inactivating component at prepulse potentials positive to −80 mV (data not shown). This was probably the result of contamination by the contribution from slowly inactivating channels, which shifted the inactivation curve to more depolarized potentials (see below). To avoid this error, data from patches with rapidly and slowly inactivating channels were not used to generate the steady-state inactivation curve of rapidly inactivating channels.

Steady-state inactivation of slowly inactivating channels was determined using the same voltage protocol as for rapidly inactivating channels. In contrast with rapidly inactivating channels, slowly inactivating channels were only partially inactivated at a prepulse potential of −40 mV and gave approximately 30% of the fully activated current when depolarized to +40 mV (Fig. 5*A* and *B*). The voltage of half-inactivation was −44 ± 9 mV ($k = 9{\cdot}5$; Table 2), in good agreement with values observed under voltage clamp for delayed rectifier current in adult *Rana* muscle (−40 mV; Adrian *et al.* 1970*a*) and the slowly inactivating potassium outward current in embryonic *Xenopus* muscle cells (−44 mV; Moody-Corbett & Gilbert, 1992).

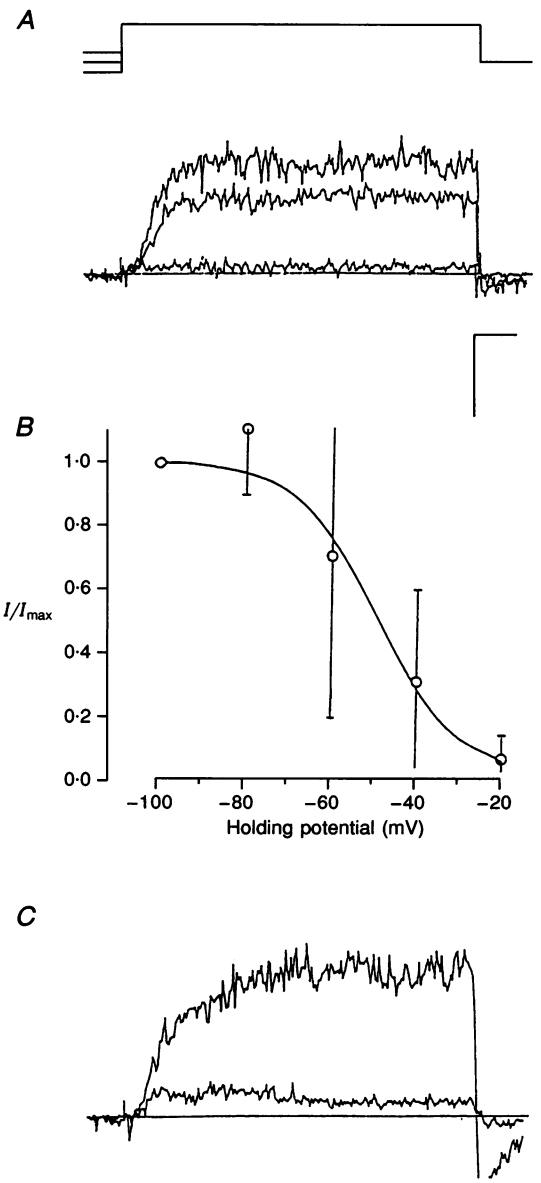

Figure 5. Slowly inactivating channels undergo steady-state inactivation

A, ensemble average currents from an excised patch decrease in amplitude with increasingly depolarized holding potentials. The patch was repeatedly stepped to +40 mV at 0·8 Hz with 50 or more steps at each potential. Holding potentials: −80, −40 and −20 mV. Horizontal scale: 2·5 ms; vertical scale: 0·5 pA. *B*, steady-state inactivation of slowly inactivating channels in cell-attached patches. Voltage protocol as in Fig. 4*B*. Data are means ± S.D. ($n = 4$). Data from periods of low open probability were omitted. *C*, open probabilities of slowly inactivating channels changed with time. Ensemble average currents from one patch obtained by repeatedly depolarizing from −100 to +40 mV at 0·8 Hz (60 or more steps each trace). The recordings of the step series giving rise to the two ensemble average currents were approximately 1 min apart. The ensemble average current with the smaller amplitude was obtained earlier after patch excision than the larger current. Scale as for *A*. Records from myocytes in enriched and mixed cultures at 20–30 h *in vitro*.

Open probability and activation of ensemble average currents

The open probabilities (P_o) of rapidly and slowly inactivating channels were assessed from ensemble average currents obtained by repeatedly depolarizing to +40 mV from a holding potential of −100 mV at 0·8 Hz. The number of channels per patch was determined from the number of superposing openings, since binomial analysis confirmed the validity of this method (see below). The open probabilities for rapidly and slowly inactivating channels were 0·28 ± 0·06 and 0·56 ± 0·08, respectively; the value for slowly inactivating channels was significantly greater than for rapidly inactivating ones in cell-attached mode (Table 2).

Open probabilities of slowly inactivating channels changed reversibly with time, when determined from ensemble average currents obtained by stepping the patch repeatedly from −100 to +40 mV (Fig. 5*C*). A decrease in P_o was correlated with clustering of traces without channel openings (not shown) as observed for delayed rectifier channels in adult *Rana* muscle (Standen, Stanfield & Ward, 1985). This was apparent when test pulses were applied every 1·2 or 3·6 s, the latter corresponding to a 2·4 s prepulse after holding at −100 mV for 1·2 s. During periods of decreased open probability, P_o was 0·14 ± 0·06 ($n = 3$). The decrease in P_o was not related to 'wash-out' or a related phenomenon, since channels residing in a low P_o mode at the onset of the recording period could switch to a higher P_o later. Three of nine slowly inactivating channels were found to reside in a low P_o mode at the start of the recording period. This phenomenon was observed in both cell-attached and excised configurations.

The rate of activation of inactivating channels depends on step potential, as evidenced by the time course of ensemble average currents at different voltages (Fig. 6). Times to half-maximal activation of ensemble average currents ($t_{½,max}$) decreased with increasing depolarization both for rapidly inactivating channels (Fig. 6*A* and *B*) and for slowly inactivating channels (Fig. 6*C* and *D*) in patches from late myocytes. In cell-attached mode, $t_{½,max}$ was significantly smaller for rapidly inactivating channels than for slowly inactivating ones (t test, $P < 0·01$; Table 2).

The activation process of both rapidly and slowly inactivating channels was slowed by patch excision. The $t_{½,max}$ of rapidly inactivating channels was significantly increased compared with the cell-attached mode immediately after patch excision (t test, $P < 0·01$; Table 2), at a time when the ensemble average currents still showed rapid inactivation (see below). A similar increase in $t_{½,max}$ was also observed for slowly

Table 2. Properties of voltage-dependent potassium channels in myocyte membrane patches 20–30 h after plating

Inactivation							
Cell attached	Excised	γ[1] (pS)	E_{rev}[1] (mV)	$V_{½}$[2] (mV)	$t_{½,max}$[3] (ms)	τ_D[4] (ms)	P_o[5]
Fast[a]	—	23 ± 6 (8)	−47 ± 19 (8)	−74 ± 7 (4)	0·79 ± 0·09 (5)	4·6 ± 2·5 (5)	0·28 ± 0·06 (5)
—	Fast[b]	23 ± 4 (5)	−41 ± 6 (5)	n.d.	1·01 ± 0·12 (8)	5·4 ± 2·1 (6)	0·23 ± 0·07 (5)
—	Slow[c]	23 ± 4 (4)	−46 ± 12 (4)	−54 ± 14† (4)	1·41 ± 0·19* (6)	675 ± 762* (7)	0·61 ± 0·14* (4)
Slow[d]	—	17 ± 4 (7)	−50 ± 9 (7)	−44 ± 9 (3)	1·17 ± 0·22 (6)	609 ± 624 (10)	0·56 ± 0·08 (4)
—	Slow[e]	18 ± 5 (5)	−50 ± 13 (5)	n.d.	1·55 ± 0·33 (7)	391 ± 304 (5)	0·57 ± 0·19 (4)

Values are given as means ± S.D. for the number of patches in parentheses. [1]Determined from linear regression of mean current amplitudes at 3 or more voltages. [2] $V_{½}$ of steady-state inactivation determined from ensemble average currents fitted with the Boltzmann relation. Holding potential, −100 mV; step potential, +40 mV. n.d., not determined. [3]Step potential, +40 mV. [4]Step potential, +40 mV. [5]Determined from ensemble average currents obtained by depolarizing voltage steps at 0·8 Hz. Holding potential, −100 mV; Step potential, +40 mV. Periods of low P_o observed for slowly inactivating channels were excluded. [a]Rapidly inactivating channels recorded in the cell-attached mode. [b]Rapidly inactivating channels recorded in the excised mode. [c]Rapidly inactivating channels in the cell-attached mode that acquired slow inactivation after patch excision. [d]Slowly inactivating channels recorded in the cell-attached mode. [e]Slowly inactivating channels recorded in the excised mode, which previously showed slow inactivation in the cell-attached mode. *Significantly different from rapidly inactivating channels (t test, $P < 0·05$), but not from slowly inactivating channels (t test, $P > 0·3$). †Significantly different from rapidly inactivating channels (t test, $P < 0·02$), but not from slowly inactivating channels ((t test, $P > 0·4$), as determined with the 0·8 Hz protocol without prepulse (data not shown).

inactivating channels after patch excision (t test, $P < 0{\cdot}05$).

Stability of channel properties

Changes in inactivation rates and other properties of ensemble average currents following patch excision

Inactivation behaviour of rapidly and slowly inactivating channels in a given patch was constant during periods of recording from cell-attached patches. In all eight patches from late myocytes recorded in this mode, the decay of ensemble average currents was unchanged after 30 min. In four of these patches, the decay of ensemble average currents was exclusively of the rapid type; in one patch, current decay was slow, and in three patches ensemble average currents had both rapid and slow components. In two of the latter cases, the relative amplitudes of fast and slow components varied between pulse series, which may have been the result of reversible shifts in open probability of slowly inactivating channels.

Inactivation behaviour of rapidly inactivating channels changes in excised inside-out patches. In fifteen of sixteen patches from late myocytes containing rapidly inactivating potassium channels immediately after patch excision, slowly inactivating channels became active within 30 min, as rapidly inactivating ones disappeared (Fig. 7*A*). The time course of this change was variable, ranging from 3 to 30 min. Since switching of voltage-dependent potassium channels between rapidly and

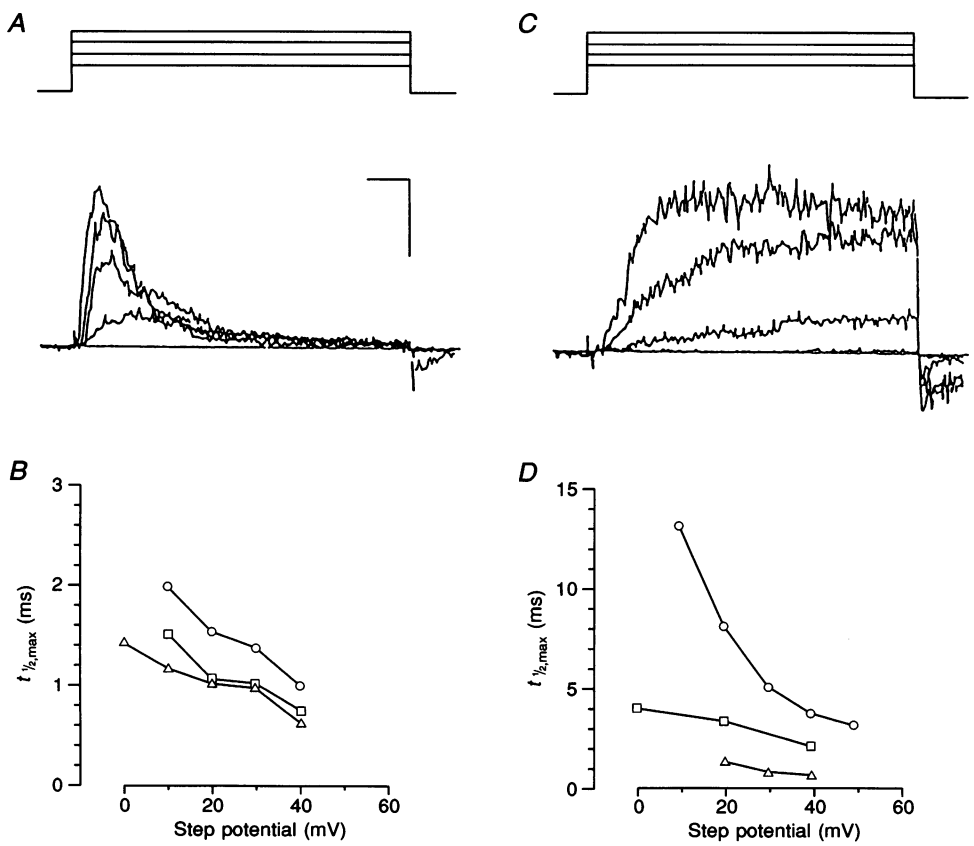

Figure 6. Activation times of ensemble average currents decrease with increasing depolarization and differ for rapidly and slowly inactivating channels

A and *B*, rapidly inactivating channels. *A*, ensemble average currents from an excised patch containing 4 rapidly inactivating channels (60 or more steps at each potential, 0·8 Hz). The patch was depolarized from −80 to 0, +20, +30 and +40 mV. *B*, time to half-maximal activation of ensemble average currents ($t_{½,max}$) as a function of voltage for channels with rapid inactivation recorded in excised configuration. Data from 3 different patches from myocytes in mixed cultures at 20–30 h *in vitro* (*A* and *B*). *C* and *D*, slowly inactivating channels. *C*, ensemble average currents from an excised patch containing 2 slowly inactivating channels (100 or more steps). The patch was depolarized from −100 to −20, 0, +20, and +40 mV. *D*, time to half-maximal activation of ensemble average currents ($t_{½,max}$) as a function of voltage for channels with slow inactivation recorded in excised configuration. Data from 3 different patches from myocytes in enriched cultures at 20–30 h *in vitro* (*C* and *D*). Horizontal scale: 2·5 ms; vertical scale: 1 (*A*) or 0·5 pA (*C*).

slowly inactivating modes has been reported in rat nodose neurones (Cooper & Shrier, 1989), we sought evidence for mode switching in channels from *Xenopus* myocytes. For patches in which slowly inactivating channels seemed to replace rapidly inactivating ones, current amplitudes of 'disappearing' channels were strikingly similar to amplitudes of newly 'appearing' channels (Figs 7*B* and 8*B*), as were their conductances and reversal potentials. This would not be expected if slowly inactivating channels were independent of rapidly inactivating ones since conductances were variable for both channel types (see above). In fact, in patches showing ensemble average currents with a decay composed of a fast and a slow component immediately after patch excision, rapidly and slowly inactivating channels displayed the expected variability in unitary current amplitude (Fig. 8*A*).

To test the independence of channel conductances statistically, the difference in amplitudes of rapidly and slowly inactivating channels was determined at +40 mV in excised patches. For cases in which both channel types were simultaneously present immediately after patch excision the difference in amplitude of rapidly and slowly inactivating channels was scattered largely between ± 1 pA with a mean of $0{\cdot}03 \pm 0{\cdot}54$ pA ($n = 11$; Fig. 8*B*). This result was expected if channel types clustered independently and the mean conductance of channel classes was not significantly different. For cases in which rapidly inactivating channels disappeared and slowly inactivating channels became active, the difference in amplitude between the two activities was less variable, ranging from 0 to $-0{\cdot}3$ pA with a mean of $-0{\cdot}12 \pm 0{\cdot}11$ pA ($n = 7$). The normal distribution could not be rejected for either set of data ($P > 0{\cdot}2$) using the Kolmogorov–Smirnov test for goodness-of-fit, and variances of the two sets of results were significantly different (F test, $P < 0{\cdot}01$). Thus, the change from rapidly to slowly inactivating channels after patch excision was considered to reflect a change in channel properties rather than the appearance of new channels.

The change in inactivation rate of rapidly inactivating channels upon patch excision was accompanied by changes in other parameters (Table 2). The voltage of half-inactivation shifted from -74 ± 7 to -54 ± 14 mV, which was not different from that of channels showing slow inactivation in cell-attached mode (t test, $P > 0{\cdot}4$). The $t_{½,\max}$ and open probability of rapidly inactivating channels also increased when inactivation of the excised channels became slow, and values were attained that were not different from those of channels initially showing slow inactivation (t test, $P > 0{\cdot}3$). Fluctuations in open probability were also observed for slow channels following conversion from rapid channels, as noted for initially slow channels (data not shown).

Reversal of the change in inactivation

The change in inactivation of rapidly inactivating potassium channels in differentiating myocytes was

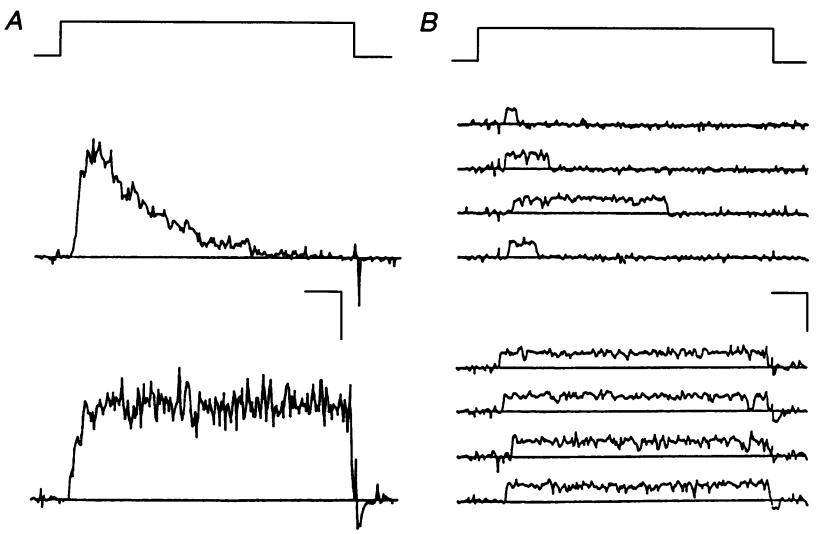

Figure 7. Rapidly inactivating channels turn into slowly inactivating ones after patch excision

A, ensemble average currents from an excised patch 1 min (upper trace) and 10 min (lower trace) after patch excision (lower trace), obtained by repeatedly depolarizing from −120 to +40 mV (60 or more steps, 0·8 Hz). Note that immediately after patch excision the ensemble average current lacks a slowly inactivating component. *B*, single-channel traces from the same patch and pulse series at the times shown in *A*. The shift from fast to slow inactivation is accompanied by little if any change in amplitude of unitary currents. Horizontal scale: 2·5 ms; vertical scale: 0·5 (*A*) or 5 pA (*B*). Records from a myocyte in an enriched culture at 25 h *in vitro*.

reversed by application of reduced dithiothreitol (DTT; Fig. 9). In all of eight patches from late myocytes, perfusion with 5 mM reduced DTT on the cytoplasmic face of inside-out patches restored rapid inactivation within seconds; DTT was effective at 1 mM in only one of three patches. Oxidized DTT at 5 or 10 mM did not reverse the change in inactivation ($n = 3$). In two patches oxidized DTT was applied at a time after patch excision when the change in inactivation was only partial, as evidenced by the presence of sweeps with rapidly and slowly inactivating channel activity. The application of 5 or 10 mM oxidized DTT completed the change to slow inactivation within less than 1 min in these instances (data not shown), indicating that oxidized DTT may accelerate the change in inactivation seen after patch excision. A similar change in inactivation behaviour has been reported for voltage-dependent potassium currents from several cloned potassium channels expressed in *Xenopus* oocytes (Ruppersberg, Stocker, Pongs, Heinemann, Frank & Koenen, 1991). The change to slow

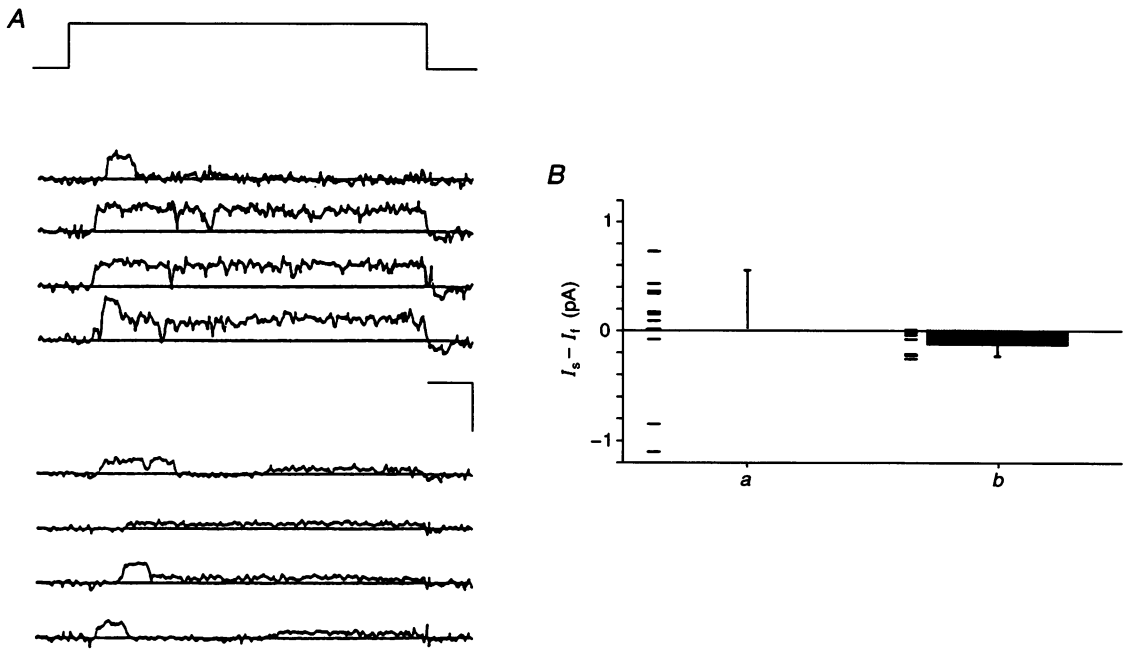

Figure 8. Rapidly inactivating channels that change kinetics do not change conductance following patch excision

A, single-channel currents from two excised patches, each containing rapidly and slowly inactivating channels active during the same recording period. Four current traces from a patch containing channels of similar conductance (upper 4 traces). Note superimposed openings of channels in the lowermost current trace. The patch was depolarized from −90 to +40 mV. Four recordings of a patch containing channels with different conductances (lower 4 traces). The patch was depolarized from −120 to +40 mV. Records from myocytes in mixed cultures at 25 and 28 h *in vitro*. Horizontal scale: 2·5 ms; vertical scale: 5 pA. *B*, the unitary current amplitude of rapidly inactivating channels (I_f) was subtracted from the unitary current amplitude of slowly inactivating channels (I_s) for individual patches and the calculated differences for the patches analysed are indicated by the horizontal bars. *a*, data from 11 patches in which the ensemble average current had rapidly and slowly inactivating components contributed by rapidly and slowly inactivating channels as shown in *A*. Averaging the differences from all patches analysed gives a mean difference of 0·03 pA. The standard deviation (0·54 pA) is indicated by the vertical bar. When rapidly and slowly inactivating channels had similar amplitudes, those for rapidly inactivating channels were determined from current traces that showed channel openings only at the beginning of the voltage step. Those for slowly inactivating channels were determined from openings at the end of the step. *b*, data from 7 patches which had rapidly inactivating ensemble average currents immediately after patch excision and slowly inactivating currents ~10 min later as shown in Fig. 7. For individual patches, the unitary current amplitude determined while the channel was rapidly inactivating was subtracted from the unitary current amplitude after the channel had switched to slow inactivation. Averaging the differences from all patches analysed gives a mean difference of −0·12 pA, and a standard deviation of 0·11 pA which is indicated by the vertical bar. Records from myocytes in mixed and enriched cultures at 20–30 h *in vitro*.

inactivation was shown to be due to oxidation of a cysteine residue in the *N*-terminal region of channel subunits and was reversed by application of DTT.

Inactivation remained slow when reduced DTT was applied to the cytoplasmic face of excised patches from late myocytes containing channels that were slowly inactivating in cell-attached configuration. No rapid inactivation was induced in six patches treated with 5 mM DTT and three patches treated with 10 mM DTT for periods of up to several minutes (data not shown). These observations suggest that a structural difference exists between rapidly inactivating channels and those that are slowly inactivating in cell-attached mode.

Clustering of channels

The number of channels per patch was determined from the number of superposing channel openings obtained with a series of 60–120 depolarizing pulses from holding potentials of −120 or −100 to +40 mV. In addition, the number of active channels was determined with binomial analysis (Patlak & Horn, 1982) from idealized current traces for patches in which the decay of ensemble average currents could be fitted by a single exponential. We used the maximum likelihood estimator (MLE) to determine the most likely number of channels in a patch. For patches with slowly inactivating channels, the MLE agreed well with the number of superposing channel openings (Fig. 10*A* and *B*). The MLE may fail, however, for low open probabilities of channels (Olkin, Petkau & Zidek, 1981). Open probabilities for rapidly inactivating channels at +40 mV generally ranged between 0·2 and 0·3 when ensemble average currents reached their peak, declining rapidly thereafter. Binomial analysis using the MLE gave the same number of channels inferred from the number of superposing channel openings, when $P_o > \sim 0{\cdot}03$ ($n = 5$ patches; Fig. 10*B* and *C*). When P_o

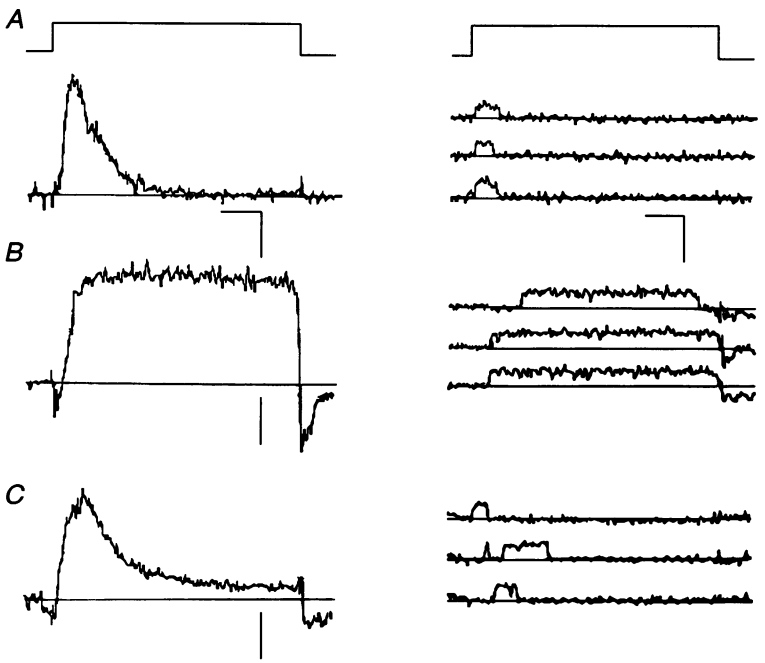

Figure 9. DTT reverses the change of inactivation behaviour of rapidly inactivating channels after patch excision

Left column. *A*, ensemble average current from a patch with 4 rapidly inactivating channels recorded in cell-attached configuration. The patch was repeatedly depolarized from −100 to +40 mV (58 steps, 0·8 Hz). *B*, after excision, channels in this patch showed slow inactivation (68 steps, 0·8 Hz). Note the apparent lack of inactivation during 20 ms steps. *C*, perfusion with 1 mM reduced DTT on the cytoplasmic side of the inside-out patch largely restored rapid inactivation and reduced open probability to the level seen in cell-attached configuration. Horizontal scale: 5 ms; vertical scale: 2 (*A* and *C*) or 5 pA (*B*). Right column: representative single-channel openings from the same patch as shown on the left, selected from those used to generate the ensemble average currents. The conductances of the channels were similar and therefore not determined individually. *A*, rapid inactivation of the channels in the cell-attached configuration. *B*, after patch excision, all 4 channels remained active and switched to slow inactivation. *C*, after perfusion with 1 mM reduced DTT, channels inactivated rapidly in the majority of cases. Occasional slow inactivation (not shown as single-channel currents) contributed a small, slowly inactivating component to the ensemble average current. All 4 channels remained active during this period. Records from a myocyte in an enriched culture at 28 h *in vitro*.

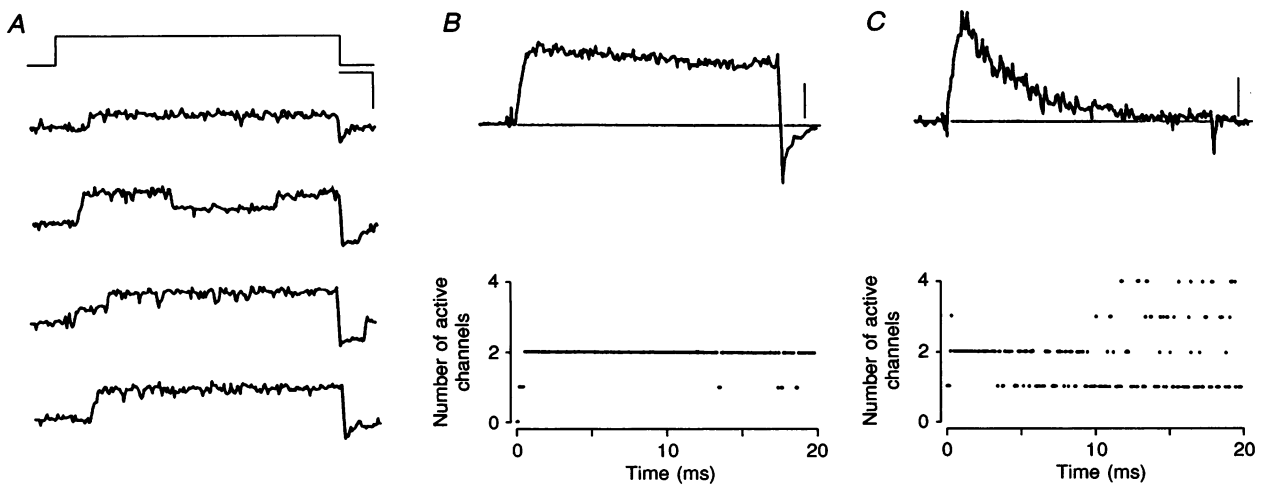

Figure 10. Binomial analysis provides an estimate of the number of active channels in patches

A, activity of two slowly inactivating channels from an excised patch during depolarizing steps from −100 to +40 mV. *B*, upper panel: ensemble average current for the patch shown in *A* (60 steps). Lower panel: the maximum likelihood estimate for the number of channels in the patch calculated for each time point separately. This estimate of two is in agreement with observation of the number of superposing channel levels. *C*, upper panel: ensemble average current for a cell-attached patch with rapidly inactivating channels (80 steps from −100 to +50 mV). Lower panel: the maximum likelihood estimate for the number of channels in the patch. During the first 10 ms, when the open probability of channels is >0·03 (based on the assumption of 2 active channels in the patch), the estimate is relatively stable and agrees with the observation of up to 2 superposing channel openings in the current traces (not shown). Thereafter the result of maximum likelihood estimation becomes unstable. Horizontal scale: 2·5 ms; vertical scale: 5 (*A*), 1 (*B*) or 0·35 pA (*C*). Records from myocytes in mixed cultures at 23 h *in vitro*.

dropped below 0·03, the prediction by the MLE became unstable (Fig. 10*C*). Therefore, we subsequently relied on the numbers obtained by inspection of current traces for superposing levels of openings.

Superposing levels of channel activity indicate the presence of more than one channel in the majority of patches showing active channels. In patches from late myocytes grown in the presence of neurones, 54% ($n = 35$) of cell-attached patches showed activity of potassium channels with rapid or slow inactivation. In 88% ($n = 17$) of patches with active channels, more than one conductance level of channel activity was observed. Clustering of channels was particularly clear in individual patches in which the number of channels was so high that it could not be reliably estimated. Such patches were recorded with pipettes of relatively high resistance

Table 3. Developmental changes in the density of potassium currents and channels for cell-attached patches in the myocyte membrane

			Channel density[b] (channels per μm^2)			
	Current density[a] (pA μm^{-2})		Early (9–12 h)		Late (20–30 h)	
Culture	Early (9–12 h)	Late (20–30 h)	Fast	Slow	Fast	Slow
Mixed	0·09 ± 0·04	1·16 ± 0·37	0·18 ± 0·12	0·11 ± 0·08	1·18 ± 0·28	0·21 ± 0·14
Enriched	0·61 ± 0·34	0·41 ± 0·18	0·92 ± 0·75	0·08 ± 0·08	0·54 ± 0·28	0·20 ± 0·10

Values are given as means ± S.D. [a]Determined by averaging amplitudes of ensemble average currents obtained by repeatedly stepping from a pipette potential of +60 to −80 mV at 0·8 Hz. Since the resting membrane potential in a bath solution containing 20 mM KCl is expected to be close to −40 mV (see Methods), holding potential is −100 mV and step potential is +40 mV across the patch membrane. The patch area is calculated from the resistance of the recording pipettes according to Sakmann & Neher (1983). Data are from 47 early and 35 late patches in mixed cultures and 41 early and 45 late patches in enriched cultures. [b]Determined from the number of superimposed levels of channel openings in the same patches used to calculate current density. Fast ($\tau_D < 25$ ms) and Slow ($\tau_D > 80$ ms) refer to the type of inactivation.

(>15 MΩ) and could contain at least ten active channels. In the majority of cases clusters were homogeneous with respect to inactivation, although patches with both channel classes were observed (e.g. Fig. 8*A*).

Clustering of channels was observed in myocytes grown in the absence of neurones, indicating that their presence was not necessary. Under these conditions, 27% ($n = 45$) of cell-attached patches of late myocytes showed channel activity and 82% ($n = 11$) of these patches showed more than one active channel.

Developmental changes in density of inactivating potassium channels

The percentage of patches with inactivating potassium channels increased with time in culture when myocytes were grown in the presence of neurones. The percentage of cell-attached patches with channel activity rose from 13% ($n = 47$) after 9–12 h to 54% ($n = 35$) after 20–30 h in culture. The increase in percentage of patches with channel activity was reflected in the increase in current density, as calculated from the amplitude of ensemble average currents, as well as in an increase in channel density (Table 3). In these cultures, the current at 2 ms after depolarization from a holding potential at which channels do not show steady-state inactivation increased 10-fold during the first day in culture. This increase was similar to the increase in channel density, indicating that the increase in amplitude of the current can be accounted for largely on this basis.

When myocytes were grown in the absence of neurones, current and channel densities decreased by roughly 30% rather than increasing during the first day in culture (Table 3). The unexpectedly high density of channels in early myocytes grown in the absence of neurones was due to a high density of rapidly inactivating channels, which decreased subsequently. The downregulation of the density of rapidly inactivating channels, which was opposite to that seen in myocytes grown in the presence of neurones, was also in contrast to developmental changes seen for slowly inactivating channels. The density of the latter channel type increased to a similar extent in myocytes grown in the absence and the presence of differentiating neurones.

DISCUSSION

Different channel classes expressed in cultured myocytes

Voltage-dependent potassium channels of *Xenopus* myocytes differentiating *in vitro* were activated by depolarization and inactivated with highly different time courses. These observations provoke the question of how many classes of potassium channels carrying outward currents are expressed during differentiation of myocytes. During extended recording periods in cell-attached configuration, inactivation behaviour of individual channels remains stable. Rapidly and slowly inactivating channels in cell-attached configuration seem to constitute two functionally distinct populations of channels which generate repolarizing currents with different kinetics during extended depolarization of the cell membrane. This interpretation is corroborated by the observation that the two classes of channels can be distinguished on the basis of other biophysical properties and are regulated differently during development.

After patch excision, however, channels with rapid inactivation generally acquired slow inactivation. Whereas properties of rapidly inactivating channels before and immediately after patch excision are similar (Table 2), the shift in behaviour with time leads to several changes. Steady-state inactivation, activation times and open probabilities also switch to resemble those of channels with natively slow inactivation. The change in inactivation behaviour after patch excision appears largely unidirectional, from rapid to slow inactivation. These results raise the possibility that a post-translational modification induces the switch in channel properties. Reduction of cysteine residues has been shown to cause such a change in several but not all cloned potassium channels (Ruppersberg *et al.* 1991). In the present study, the change from rapid to slow inactivation after patch excision could be reversed by application of the reducing form of dithiothreitol (DTT), similar to observations with RCK4 (rat Kv1.4) and Raw3 (rat Kv3.4) potassium channels.

Channels which were slowly inactivating before and after patch excision were not converted to rapidly inactivating channels by application of DTT to the cytoplasmic face of the membrane. This result suggests a molecular difference between these two channel classes, and implies that channels that already inactivate slowly in cell-attached mode lack the site responsive to the reducing reagent or possess this site in a manner protected against reduction. The pore-forming subunits of the two channel classes may be derived from different genes or from a single gene. In the latter case, a stable modification is required to generate different inactivation behaviour, such as the alteration of an amino acid side chain or the binding of a regulatory subunit. The phosphorylation state of *Shaker* channels (Drain, Dubin & Aldrich, 1994) and the association with β-subunits of *Shaker*-related rat potassium channels (Rettig *et al.* 1994) are effective in changing the inactivation behaviour of the channels. The similarity of properties of natively slow channels and channels which switch from rapid to slow inactivation after patch excision in *Xenopus* myocytes suggests that the channels are structurally related. Whether they are derived from a single gene will be decided by molecular techniques.

Comparison with voltage-dependent potassium channels in frog muscle

The properties of potassium currents have been intensively investigated in muscle of mature frogs. Voltage-dependent delayed rectifier outward currents of *Rana* inactivated completely during extended depolarizing voltage commands (Adrian *et al.* 1970*a*; Adrian, Chandler & Hodgkin, 1970*b*; Stanfield, 1970). The voltage of half-inactivation was reported to be close to −40 mV (Adrian *et al.* 1970*a*). Two components were distinguished by current decay (Stanfield, 1970) as well as by activation and deactivation kinetics (Adrian *et al.* 1970*b*). In single-channel recordings on vesicles from frog muscle membrane, voltage-dependent potassium-selective channels with a conductance of 15 pS in physiological $[K^+]_o$ have been described (Standen *et al.* 1984, 1985). These channels showed properties expected for channels underlying the delayed-rectifier currents recorded in frog muscle. Slow inactivation upon prolonged voltage steps can be inferred from the ensemble average currents (Standen *et al.* 1985).

The conductance, ion selectivity and inactivation of slowly inactivating channels in membranes from *Xenopus* myocytes differentiating *in vitro* (this study) agree with those found in striated muscle of adult *Rana* (Standen *et al.* 1984, 1985). In addition, steady-state inactivation of the delayed rectifier-like currents (Adrian *et al.* 1970*a*) and the slowly inactivating channels described here are similar. Decay of whole-cell currents in adult frog muscle was described as having fast and slow components with time constants of ~270 ms and ~2·3 s, depending on recording conditions (Stanfield, 1970; Adrian *et al.* 1970*a*). Our value of 600 ms may not be directly comparable with these results, since it is an average from many patches with variable decay time constants ranging from 80 to 2000 ms.

A rapidly inactivating current in embryonic *Xenopus* myocytes (Ribera & Spitzer, 1991; Moody-Corbett & Gilbert, 1992; Spruce & Moody, 1992) is generated by a different channel class (this study). It remains to be determined whether the lack of this channel class in adult *Rana* muscle (Adrian *et al.* 1970*a*, *b*; Stanfield, 1970; Standen *et al.* 1984, 1985) is due to differences in species or developmental stage.

The properties of inactivating potassium channels recorded in membrane patches from *Xenopus* myocytes differentiating *in vitro* account qualitatively for the outward potassium currents recorded in the whole-cell configuration (Ribera & Spitzer, 1991; Moody-Corbett & Gilbert, 1992; Spruce & Moody, 1992). A quantitative comparison is difficult due to the shift of rapidly inactivating channels from fast to slow inactivation after patch excision in an oxidizing environment. Assuming that this shift also occurs in the whole-cell configuration when the pipette solution does not contain a reducing agent, the density of the slowly inactivating current in the whole-cell configuration is similar to the current density obtained from single-channel recording. The comparison entails extrapolation of the density of delayed rectifier current recorded from *Xenopus* myocytes in mixed cultures (Ribera & Spitzer, 1991) to a step potential of +40 mV, and consideration of steady-state inactivation to 30% of full channel availability at a holding potential of −40 mV for channels with slow inactivation (this study). On this basis, the densities of whole-cell delayed rectifier currents were 0·17 and 1·12 pA μm^{-2} for early and late myocytes when elicited from a holding potential of −120 mV. These values are in reasonable agreement with densities of 0·09 and 1·16 pA μm^{-2} obtained from single-channel recording. The $t_{½,max}$ of whole-cell current extrapolated to +40 mV is also in agreement with the value obtained from single-channel recording of slowly inactivating channels in late myocytes. However, a difference between current density in whole-cell (Ribera & Spitzer, 1991; Spruce & Moody, 1992) and single-channel recording may exist in myocyte-enriched cultures from which neurones are absent. The current densities obtained from single-channel recording at early stages are larger than those obtained from whole-cell recording after accounting for step potential and steady-state inactivation. The disparities could be due to a difference in channel distribution.

Comparison with voltage-dependent potassium channels in other preparations

Potassium channels were first cloned from the *Shaker* locus in *Drosophila* (for review see Jan & Jan, 1992). The *Shaker* mutation affects transient potassium A currents while sparing delayed rectifier currents in *Drosophila* muscle cells *in vivo* (Salkoff & Wyman, 1981, 1983) and *in vitro* (Zagotta & Aldrich, 1990). Several classes of voltage-dependent potassium channels have been observed in embryonic *Drosophila* muscle cells differentiating in culture (Zagotta, Brainard & Aldrich, 1988). The A_1 channel with a conductance of 13–16 pS in excised configuration resembles the rapidly inactivating channel described in the present study. Interestingly, the *Drosophila* channel shows increased variability in rate of inactivation when recorded in excised configuration (Zagotta *et al.* 1988). However, expression of cloned *Shaker* channels in *Xenopus* oocytes demonstrates that they do not change from rapid to slow inactivation after patch excision. They lack the cysteine residue that mediates sensitivity of inactivation to reducing agents in other potassium channels such as RCK and Raw (Ruppersberg *et al.* 1991) and possibly the rapidly inactivating channel in *Xenopus* muscle (this study). The K_D channel in differentiating *Drosophila* muscle cells, with a conductance of 11–16 pS, inactivates during long

depolarizing steps (Zagotta *et al.* 1988). This channel, which resembles the slowly inactivating channel in *Xenopus* myocytes (this study), is not affected by a *Shaker* mutation and is thought to be derived from an as yet uncharacterized gene.

Transient potassium channels with variable inactivation rates have also been observed in different neuronal preparations. In rat nodose neurones, inactivation behaviour of channels in cell-attached multichannel patches was reported to change with time, indicating possible switching between rapidly and slowly inactivating modes (Cooper & Shrier, 1989).

Mode switching in voltage-dependent ion channels

Changes in gating modes have been described for voltage-dependent sodium and calcium channels. Clustering of sweeps without activity in recordings of sodium channels in outside-out patches from GH_3 cells was considered due to a slow cycling between an activatable and a non-activatable state, termed 'hibernation' (Horn, Vandenberg & Lange, 1984). A similar behaviour was observed in voltage-dependent calcium channels recorded in cell-attached patches of guinea-pig cardiac cells (Hess, Lansman & Tsien, 1984; Cavalie, Pelzer & Trautwein, 1986).

In differentiating *Xenopus* myocytes, slowly inactivating potassium channels show variable open probability at the same test potential presented at 0·28 Hz. Non-random ordering of traces with or without channel activity was also observed in recordings of single delayed rectifier channels from adult *Rana* muscle (Standen *et al.* 1985). Thus, the clustering of traces without channel openings as well as the change in open probabilities for pulse series at a given voltage protocol may represent a slow reversible change in channel properties like that described for sodium and calcium channels.

Changes in inactivation behaviour of voltage-dependent sodium and calcium channels have also been described (Patlak & Ortiz, 1985, 1989; Plummer & Hess, 1991). Sodium channels from rat heart muscle cells showed fast as well as slow inactivation, which was considered to be due to one channel class operating in different 'modes' rather than two different channel classes (Patlak & Ortiz, 1985, 1989). Such behaviour has also been shown for cloned rat brain sodium channels expressed in *Xenopus* oocytes (Moorman, Kirsch, VanDongen, Joho & Brown, 1990). In comparison with calcium channels, slow inactivation of sodium channels occurs infrequently. After patch excision, slow inactivation may become prevalent in sodium channels from guinea-pig and rat heart cells (Nilius, 1988; Kirsch & Brown, 1989), but not, however, in rat neocortical cells (Kirsch & Brown, 1989). The finding that such a change in inactivation behaviour is observed after patch excision in some but not all voltage-dependent potassium channels (Ruppersberg *et al.* 1991; this study) suggests a structural as well as a functional similarity between sodium, calcium and potassium channels. Considering the slow cycling between gating modes, it was suggested that a reversible covalent modification is responsible for this phenomenon (Plummer & Hess, 1991). Redox modification of a cysteine residue in the *N*-terminal region of potassium channels is one possibility; changing the phosphorylation state of channel proteins (Drain *et al.* 1994) as well as interaction with different regulatory subunits (Rettig *et al.* 1994) may be physiologically relevant ways to achieve a shift between gating modes. Together with the existence of several genes encoding each class of voltage-dependent ion channels and the opportunity for alternative splicing, an enormous regulatory potential is available during differentiation of excitable cells.

Adrian, R. H., Chandler, W. K. & Hodgkin, A. L. (1970*a*). Voltage clamp experiments in striated muscle fibres. *Journal of Physiology* **208**, 607–644.

Adrian, R. H., Chandler, W. K. & Hodgkin, A. L. (1970*b*). Slow changes in potassium permeability in skeletal muscle. *Journal of Physiology* **208**, 645–668.

Byrkin, D. R. (1987). *Statistics Today.* Benjamin/Cummings Publishing Company, Inc., Menlo Park, CA, USA.

Cavalie, A., Pelzer, D. & Trautwein, W. (1986). Fast and slow gating behaviour of single calcium channels in cardiac cells. *Pflügers Archiv* **406**, 241–258.

Cooper, E. & Shrier, A. (1989). Inactivation of A currents and A channels on rat nodose neurons in culture. *Journal of General Physiology* **94**, 881–910.

Daniel, W. W. (1978). *Biostatistics: A Foundation For Analysis in the Health Sciences*, 2nd edn. John Wiley and Sons, New York.

Drain, P., Dubin, A. E. & Aldrich, R. W. (1994). Regulation of *Shaker* K^+ channel inactivation gating by the cAMP-dependent protein kinase. *Neuron* **12**, 1097–1109.

Ernsberger, U. & Spitzer, N. C. (1990). Expression of potassium A current channels in *Xenopus* myocytes during differentiation in culture. *Society for Neuroscience Abstracts* **16**, 507.

Ernsberger, U. & Spitzer, N. C. (1991). *Xenopus* myocytes differentiating *in vitro* express several classes of transient potassium channels. *Society for Neuroscience Abstracts* **17**, 1475.

Harris, G. L., Henderson, L. P. & Spitzer, N. C. (1988). Changes in densities and kinetics of delayed rectifier potassium channels during neuronal differentiation. *Neuron* **1**, 739–750.

Hess, P., Lansman, J. B. & Tsien, R. W. (1984). Different modes of Ca channel gating behaviour favoured by dihydropyridine Ca agonists and antagonists. *Nature* **311**, 538–544.

Horn, R., Vandenberg, C. A. & Lange, K. (1984). Statistical analysis of single sodium channels. *Biophysical Journal* **45**, 323–335.

Howe, J. R. & Ritchie, J. M. (1991). On the active form of 4-aminopyridine: block of K^+ currents in rabbit Schwann cells. *Journal of Physiology* **433**, 183–205.

HUSSY, N. (1991). Developmental change in calcium-activated chloride current during the differentiation of *Xenopus* spinal neurons in culture. *Developmental Biology* **147**, 225–238.

JAN, L. Y. & JAN, Y. N. (1992). Structural elements involved in specific K^+ channel functions. *Annual Review of Physiology* **54**, 537–555.

KIRSCH, G. E. & BROWN, A. M. (1989). Kinetic properties of single sodium channels in rat heart and rat brain. *Journal of General Physiology* **93**, 85–99.

MOODY-CORBETT, F. & GILBERT, R. (1992). A K^+ current in *Xenopus* muscle cells which shows inactivation. *Neuroreport* **3**, 153–156.

MOORMAN, J. R., KIRSCH, G. E., VANDONGEN, A. M. J., JOHO, R. H. & BROWN, A. M. (1990). Fast and slow gating of sodium channels encoded by a single mRNA. *Neuron* **4**, 243–252.

NIEUWKOOP, P. D. & FABER, J. (1956). Normal table of *Xenopus laevis* (Daudin). North Holland Publishing, Amsterdam.

NILIUS, B. (1988). Modal gating behavior of cardiac sodium channels in cell-free membrane patches. *Biophysical Journal* **53**, 857–862.

OLKIN, I., PETKAU, A. J. & ZIDEK, J. V. (1981). A comparison of n estimates for the binomial distribution. *Journal of the American Statistical Association* **76**, 637–642.

PATLAK, J. B. & HORN, R. (1982). Effects of *N*-bromoacetamide on single sodium channel currents in excised membrane patches. *Journal of General Physiology* **79**, 333–351.

PATLAK, J. B. & ORTIZ, M. (1985). Slow currents through single sodium channels in the adult rat heart. *Journal of General Physiology* **86**, 89–104.

PATLAK, J. B. & ORTIZ, M. (1989). Kinetic diversity of Na^+ channel bursts in frog skeletal muscle. *Journal of General Physiology* **94**, 279–301.

PLUMMER, M. R. & HESS, P. (1991). Reversible uncoupling of inactivation in *N*-type calcium channels. *Nature* **351**, 657–659.

RETTIG, J., HEINEMANN, S. H., WUNDER, F., LORRA, C., PARCEJ, D. N., DOLLY, J. O. & PONGS, O. (1994). Inactivation properties of voltage-gated K^+ channels altered by presence of β-subunit. *Nature* **369**, 289–294.

RIBERA, A. & SPITZER, N. C. (1991). Differentiation of delayed rectifier potassium current in embryonic amphibian myocytes. *Developmental Biology* **144**, 119–128.

RUDY, B. (1988). Diversity and ubiquity of K channels. *Neuroscience* **25**, 729–750.

RUPPERSBERG, J. P., STOCKER, M., PONGS, O., HEINEMANN, S. H., FRANK, F. & KOENEN, M. (1991). Regulation of fast inactivation of cloned mammalian I_K(A) channels by cysteine oxidation. *Nature* **352**, 711–714.

SAKMANN, B. & NEHER, E. (1983). Geometric parameters of pipettes and membrane patches. In *Single-Channel Recording*, ed. SAKMANN, B. & NEHER, E., pp. 37–51. Plenum Publishing Corporation, New York.

SALKOFF, L. & WYMAN, R. (1981). Genetic modification of potassium channels in *Drosophila Shaker* mutants. *Nature* **293**, 228–230.

SALKOFF, L. B. & WYMAN, R. J. (1983). Ion currents in *Drosophila* flight muscles. *Journal of Physiology* **337**, 687–709.

SPITZER, N. C. (1976). The ionic basis of the resting potential and a slow depolarizing response in Rohon-Beard neurones of *Xenopus* tadpoles. *Journal of Physiology* **255**, 105–135.

SPRUCE, A. E. & MOODY, W. J. (1992). Developmental sequence of expression of voltage-dependent currents in embryonic *Xenopus laevis* myocytes. *Developmental Biology* **154**, 11–22.

STANDEN, N. B., STANFIELD, P. R. & WARD, T. A. (1985). Properties of single potassium channels in vesicles formed from the sarcolemma of frog skeletal muscle. *Journal of Physiology* **364**, 339–358.

STANDEN, N. B., STANFIELD, P. R., WARD, T. A. & WILSON, S. W. (1984). A new preparation for recording single-channel currents from skeletal muscle. *Proceedings of the Royal Society* B **221**, 455–464.

STANFIELD, P. R. (1970). The effect of the tetraethylammonium ion on the delayed currents of frog skeletal muscle. *Journal of Physiology* **209**, 209–229.

STÜHMER, W., RUPPERSBERG, J. P., SCHRÖTER, K. H., SAKMANN, B., STOCKER, M., GIESE, K. P., PERSCHKE, A., BAUMANN, A. & PONGS, A. (1989). Molecular basis of functional diversity of voltage-gated potassium channels in mammalian brain. *EMBO Journal* **8**, 3235–3244.

TIMPE, L. C., JAN, Y. N. & JAN, L. Y. (1988). Four cDNA clones from the *Shaker* locus of *Drosophila* induce kinetically distinct A-type potassium currents in *Xenopus* oocytes. *Neuron* **1**, 659–667.

WEI, A., COVARRUBIAS, M., BUTLER, A., BAKER, K., PAK, M. & SALKOFF, L. (1990). K^+ current diversity is produced by an extended gene family conserved in *Drosophila* and mouse. *Science* **248**, 599–603.

ZAGOTTA, W. & ALDRICH, R. (1990). Voltage-dependent gating of *Shaker* A-type potassium channels in *Drosophila* muscle. *Journal of General Physiology* **95**, 29–60.

ZAGOTTA, W., BRAINARD, M. S. & ALDRICH, R. W. (1988). Single-channel analysis of four distinct classes of potassium channels in *Drosophila* muscle. *Journal of Neuroscience* **8**, 4765–4779.

Acknowledgements

We thank Beverly Clendening, Michel Desarmenien, Xiaonan Gu, Greg Harris, Janet Holliday, Nicolas Hussy, Roger Papke, Angie Ribera and Jack Rice for helpful discussions, and also Rosario de Baca, Forrest Gompf and Steve Watt for technical assistance. This work was supported by NIH NS 25916. U.E. was a Fellow of the Muscular Dystrophy Association and of the Deutsche Forschungsgemeinschaft.

Author's present address

U. Ernsberger: Max-Planck-Institut für Hirnforschung, Deutschordenstrasse 46, 60496 Frankfurt/M, Federal Republic of Germany.

Received 4 February 1994; accepted 14 September 1994.